A COMPARISON OF BTE-BASED ELECTRON TRANSPORT SIMULATIONS FOR SILICON

J.M. Higman *
Motorola
Advanced Products Research and Development Laboratory, MD K-10
3501 Ed Bluestein Blvd., Austin, Texas 78721

ABSTRACT

A unique study of several previously reported computer simulations which solve the Boltzmann Transport Equation (BTE) for electrons in silicon has been completed. A total of 47 individuals representing 19 laboratories in 6 countries participated in this comparison, with a total of 21 data sets contributed. Most of the simulations are based on the Monte Carlo particle technique, and have been used here to calculate a set of transport characteristics for intrinsic silicon at room temperature with a homogeneous electric field. From a global perspective the results vary widely, but they provide for the first time a quantitative comparison of many silicon transport models. If we group the data sets according to their bandstructure models and compare groups to one another the separate effects of bandstructure and phonon scattering rates can be seen. In the group of full-band models we observe a striking and unexpected agreement between 4 of the data sets, and the possible significance of this observation will be discussed.

I. INTRODUCTION

In this study, initiated within the National Center for Computational Electronics, we present a comparison [1] of many of the computer simulation codes which have been developed throughout the world for simulating electron transport in silicon. A number of researchers solved the BTE (all but one using the Monte Carlo particle method) for a specific set of conditions, and the results of all of these simulations have been compiled allowing the first direct comparison of a broad spectrum of transport models. The focus of this study is on the physical models and how they might affect the calculated distributions, and not programmer-dependent qualities such as computational speed or the algorithms.

Each simulation code was used to calculate the energy distribution of electrons in homogeneous, intrinsic silicon at room temperature with time-invariant applied electric fields of 30kV/cm, 150kV/cm and 300kV/cm. For each field, the percentage of electrons above 1.1eV, 1.8eV and 3.1eV were calculated.

II. RESULTS

Each of the 21 data sets are listed after the references, with a brief description of the bandstructure model, a list references to the literature which describes the model, and the names of the contributors. It is useful to separate the data sets into three groups according to their bandstructure models, and all of the figures are organized according to this scheme. The first group (sets 1 through 7) consists of models which use effective mass bands; these are either spherical or ellipsoidal constant-energy surfaces, and can be either parabolic or nonparabolic. The second group (sets 8 through 16) contains data sets which use "fit" bandstructure models. These models differ from one another in detail but in principle they are all constructed of analytic functions which contain a number of adjustable parameters such that some properties of the full bandstructure of silicon at higher energies can be emulated, while retaining the simplicity of analytical expressions. For example, the bandstructure may be fit to the density-of-states extracted from a full bandstructure calculation. Set number 8 is included in the fit-band group although it uses only effective-mass bands, but since it uses both X- and L-valleys it is similar to the other models in this group. The

third group (sets 17 through 21) consists of the full-band Monte Carlo simulations where the $E(\mathbf{k})$ relation is calculated using the pseudopotential method, tabulated on a three-dimensional grid in $\mathbf{k}$-space, and interpolated as needed during the monte carlo simulation.

All data sets except 19, 20, and 21 use electron-phonon models based on phenomenological coupling constants. Both the acoustic deformation potential and the intervalley coupling constants are adjusted to reproduce (some) measured data. Data sets 19 through 21 represent the newest attempts at physical models for the transport without any fitting parameters *per se*. In these transport models the pseudopotential description of the crystal is used to calculate both the bandstructure and the electron-phonon interaction, thus treating the free propagation of the electron on the same footing with scattering.

Figures 1(a) through (c) show the total electron-phonon scattering rates (emission plus absorption) for the effective mass, fit-, and full-band groups of data, respectively. Although this is an incomplete representation of any particular transport model - the relative magnitudes of rates for different mechanisms and the impact ionization rate are not shown - it does give some indication about structure in the electronic density-of-states and the strength of the electron-phonon coupling used in the model. At high electric fields the impact ionization scattering rate may have a strong effect on the electron energy distribution and the details of the ionization scattering rates can be found in the references given for each data set.

Figures 2(a) through (c) show the energy distribution of electrons for 30kV/cm, for the three groups of data. Each of the three groups has one model with a much more highly populated tail than the others (sets 2, 10, and 19). The model for set number 2 uses a parabolic, spherical band resulting in a low scattering rate and large population at high energies. In order to understand Figure 2 further we use the effective deformation potential $(DK)_{ij} = [\sum_{\eta} \Delta_{\eta}^2]^{\frac{1}{2}}$ and effective phonon energy $(\hbar\omega)_{ij}^{-1} = \frac{1}{(DK)_{ij}^2} \sum_{\eta} \frac{\Delta_{\eta}^2}{\hbar\omega_{\eta}}$ for the conduction band edge, which were introduced in [14]. The subscripts ij indicate a pair of conduction band minima and Δ_{η} is the coupling constant for phonon branch η. Averaging $(DK)_{ij}$ and $(\hbar\omega)_{ij}$ over all possible minima ij give average effective scattering parameters shown for each model in Fig. 3. The arrows on Fig. 3 indicate the three apparently outlying data sets of Fig. 2, showing that these data sets have the smallest average coupling $< (DK) >$ in their respective groups. Judging from the fit- and full-band data, at lower fields (30kV/cm in this case) the electron-phonon coupling has the strongest influence on the tail of the distribution.

Figure 4 shows the three groups of data as in Figure 2, for an applied electric field of 150kV/cm. In Fig. 4(a) we see again that due to the bandstructure model used in set 2 it falls far from the nonparabolic band models. The fit-band model distributions shown in Fig. 4(b) exhibit considerable scatter in the tail populations at this intermediate field value. The consistency among the full-band models is improving as the field is increased, with set 19 still showing a much larger population at high energies.

The electron distributions for an applied electric field of 300kV/cm are shown in Figure 5. For the effective mass bands, Fig. 5(a), the non-parabolic models predict more consistent distributions than do the fit-band models of Fig. 5(b), and the agreement among the full-band models has improved over the 150kV/cm case. This observation concerning the full-band models is unexpected since the electron-phonon interaction models differ dramatically, from phenomenological coupling constants of models 17 and 18, to the pseudopotential-based, anisotropic coupling of models 19, 20, and 21, and quite different impact ionization models. This suggests that at higher electric fields the bandstructure has more influence on the electron distribution; the fit-band models, which use a variety of analytic expressions and fitting schemes to determine the bandstructure give widely varying results at higher fields. The non-parabolic, effective mass band models (excluding for the moment the spherical-parabolic model of set 2) and full-band models, which have well-defined, consistent bandstructures from one model to another, become more consistent with one another at higher fields. It is important to note that consistent results among any group of models does not necessarily indicate that they are close to the *correct* result.

Figures 6 and 7 show information about the integrated distribution, fraction of electrons above 1.1eV (near the impact ionization threshold) for an applied field of 150kV/cm, and the average energy for each data set at 150 and 300kV/cm. These figures emphasize the disagreement across all data sets, as we observe that the average energy varies by a factor of 5 at these fields (a factor which becomes *worse* at lower fields).

III. CONCLUSION

In summary, we can say that the disagreement among the results is unacceptably large, and from a global perspective the data is discouraging, but by dividing the data into groups according to the band-structure models we see that some encouraging trends exhibit themselves. In addition, the data hints at some potentially fundamental observations about the relative role of bandstructure and electron-phonon scattering in different field ranges: At higher fields the distribution is much less dependent on the details of the scattering rates and is determined largely by the bandstructure. These conclusions are tentative at best, but they indicate the kind of information that is available, and the importance of such broad-based studies.

ACKNOWLEDGMENT

The author would like to thank all of the participants for their cooperation, many of whom made valuable comments and suggestions in addition to contributing data. Thanks also to Chiang-Sheng Yao (Stanford U.) who collected and compiled the data, and to Karl Hess and Bob Dutton who supported this effort from its beginning.

* This work was done at the University of Illinois at Urbana-Champaign while the author was employed there, supported by the NSF through the National Center for Computational Electronics.

REFERENCES

1. These results were initially shown and discussed by several of the participants and others during the Workshop on Computational Electronics, May 1992, University of Illinois at Urbana-Champaign. A detailed manuscript including all contributors as authors has been submitted to *IEEE Trans. Electron Devices*
2. Th. Vogelsang, W. Haensch, J. Appl. Phys., vol. 70, pp. 1493-1499 1991.
3. J.Y. Tang and K. Hess, J. Appl. Phys., vol. 54, pp. 5193-5144, 1983.
4. R. Brunetti, C. Jacoboni, F. Venturi, E. Sangiorgi, and B. Ricco, Solid-State Elect., vol. 32, pp. 1663-1667, 1989.
5. S. Ramaswamy, MS thesis, University of Massachusetts, Amherst, 1992.
6. P.D. Yoder, J.M. Higman, J. Bude, and K. Hess, Semicond. Sci. and Technol., vol. 7, B357-B359, 1992.
7. T. Iizuka, M. Fukuma, Solid-State Electronics, vol. 33, pp. 27-34, 1990.
8. C. Jacoboni, R. Minder, and G Majni, J. Phys. Chem. Solids, vol. 36, pp. 1129-1133, 1975.
9. R. Thoma, H.J. Peifer, W.L. Engl, W. Quade, R. Brunetti, and C. Jacoboni, J. Appl. Phys., vol. 69, pp. 2300-2311, 1991.
10. H.-J. Peifer, B. Meinerzhagen, R. Thoma, and W.L. Engl, IEDM Tech. Digest, pp. 131-134, 1991.
11. C. Fiegna and E. Sangiorgi, IEEE Trans. Electron Devices, vol. ED-40, pp.619-627, 1993.
12. C. Fiegna, et al., IEDM Tech. Digest, pp. 451, 1990.
13. M.V. Fischetti and S. Laux, Phys. Rev. B, vol. 38, pp. 9721-9745 1988.
14. M.V. Fischetti, IEEE Trans. Electron Devices, vol. 38, pp. 634-649, 1991.
15. C. Jacoboni and L. Reggiani, Rev. Mod. Phys., vol. 55, pp. 645-705 1983.
16. A. Phillips, Jr., and P. J. Price, Appl. Phys. Lett., vol. 30, pp. 528-530, 1977.

17. H. Kosina and S. Selberherr, Jpn. J. Appl. Phys., vol. 29, pp. 2283-2285, 1990.
18. P. Hesto, These Doctorat es Sciences, Orsay, France 1984.
19. M. Mouis, These Doctorat es Sciences, Orsay, France, 1988.
20. H. Mizuno, K. Taniguchi, C. Hamaguchi, Semicond. Sci. Technol., vol. 7, pp. B379-B381, 1992.
21. N. Sano, M. Tomizawa, A. Yoshii, Jpn. J. Appl. Phys, vol. 30, pp. 3662-3665, 1991.
22. N. Sano and A. Yoshii, Phys. Rev. B, vol. 45, pp. 4171-4180, 1992.
23. T. Kunikiyo, T. Kamakura, M. Yamaji, H. Mizuno, M. Takenaka, K. Taniguchi, and C. Hamaguchi, Procedings of 1993 VPAD (International Workshop on VLSI Process and Device Modeling), p.40, 1993.
24. X. Wang, V. Chandramouli, C.M. Maziar, and A. F. Tasch, J. Appl. Phys., vol. 73, pp.3339-3347, 1993.
25. S.-L. Wang, N. Goldsman, K. Hennacy, J. Appl. Phys., vol. 71, pp. 1815-1822, 1992.
26. P. D. Yoder, Ph.D. Thesis, Univ. of Illinois, 1993.
27. C. Hao, J. Zimmermann, M. Charef, R. Fauquembergue, and E. Constant, Solid-State Electron., vol. 28, pp.773-740, 1985.
28. M. Charef, Thesis, Universite des Sciences et Technologies de Lille, France (1983).
29. A. Abramo, F. Venturi, E. Sangiorgi, J. Higman, and B. Ricco, IEEE Trans. Computer-Aided Design, vol. CAD-12, no.9, pp.1327-1335, September 1993.
30. C.-S. Yao, D. Chen, R. Dutton, F. Venturi, E. Sangiorgi, and A. Abramo, Procedings of 1993 VPAD (International Workshop on VLSI Process and Device Modeling), p.42, 1993.

Data Sets

1. The first three Legendre polynomials are used [15,25]. (Goldsman, Hennacy, Lin, S.-L. Wang)
2. Parbolic, spherical band model, six equivalent valleys [18,19]. (Hesto, Galdin, Dollfus, Castagne)
3. Non-parabolic, ellipsoidal band model [15,16,17]. (Kosina, Hackel, Selberherr)
4. Non-parabolic, ellipsoidal band model [40]. (K. Tomizawa)
5. Non-parabolic, ellipsoidal band model [27,28]. (Charef, DEssenne, Thobel, Baudry, Fauquembergue)
6. Non-parabolic, ellipsoidal band model [5]. (Ramaswamy, Tang)
7. Non-parabolic, ellipsoidal band model [7,8]. (Iizuka)
8. Non-parabolic, ellipsoidal band model for X-valleys, parabolic, spherical band model for L-valleys [21,22]. (Sano, M. Tomizawa, Yoshii)
9. Anaylytic fit band model [4,24]. (Wang, Maziar)
10. Analytic fit band model [2]. (Vogelsang)
11. Analytic fit band model [4]. (Scrobohaci, Tang)
12. Analytic fit band model [4,9,10]. (Peifer, Thoma, Jungemann, Engl)
13. Analytic fit band model [4,11]. (Fiegna, Brunetti)
14. Analytic fit band model [4,11,12]. (Fiegna)
15. Analytic fit band model [20]. (Mizuno, Taniguchi, Hamaguchi)
16. Analytic fit band model [29,30]. (Abramo, Yao)
17. Full band model [3,36,41]. (Higman, Hess)
18. Full band model [13,14]. (Fischetti, Laux)
19. Full band model [6]; no adjustable electron-phonon parameters in this model. (Yoder, Higman, Hess)
20. Full band model [23]; no adjustable electron-phonon parameters in this model. (Kunikiyo, Mizuno, Kamakura, Takenaka, Taniguchi, Hamaguchi)
21. Full band model [26]; no adjustable electron-phonon parameters in this model. (Yoder, Hess)

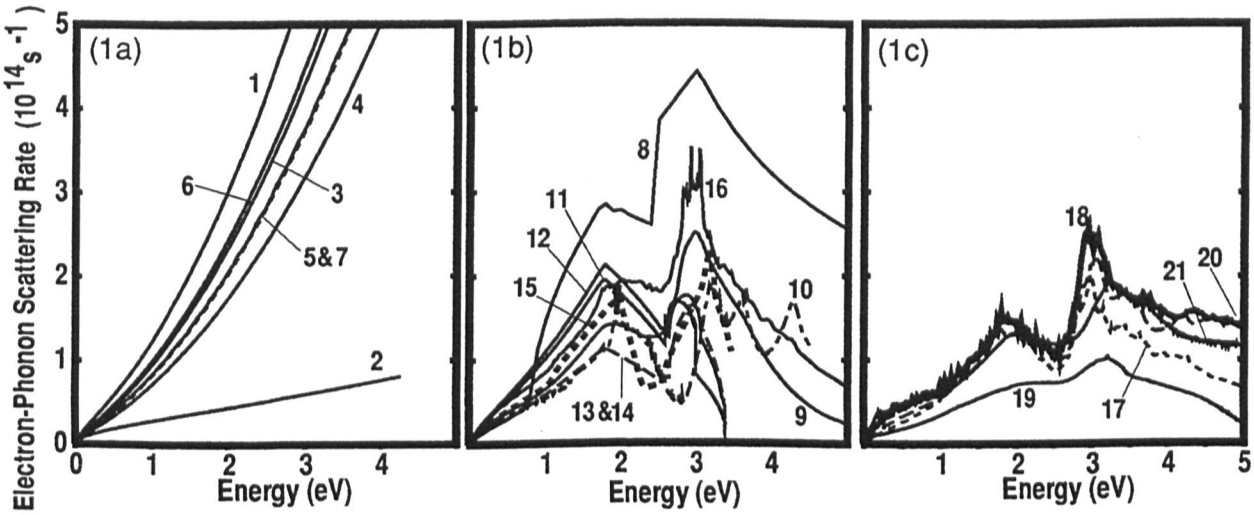

Figure 1. Electron-phonon scattering rates for (a) effective mass band models, (b) fit-band models, and (c) full-band models.

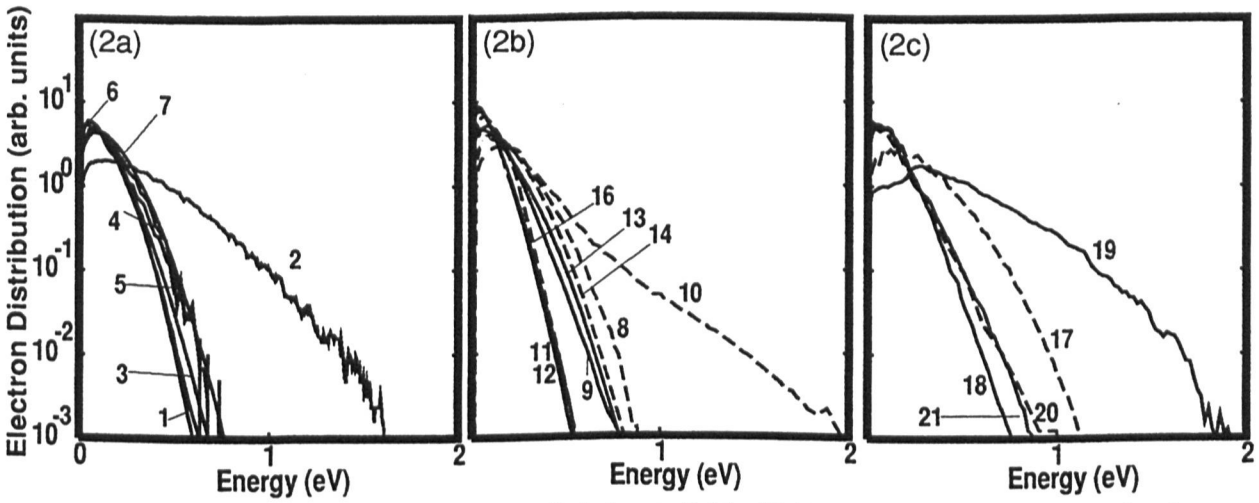

Figure 2. Electron distribution for an applied electric field = 30 kV/cm, for (a) effective mass band models, (b) fit-band models, and (c) full-band models.

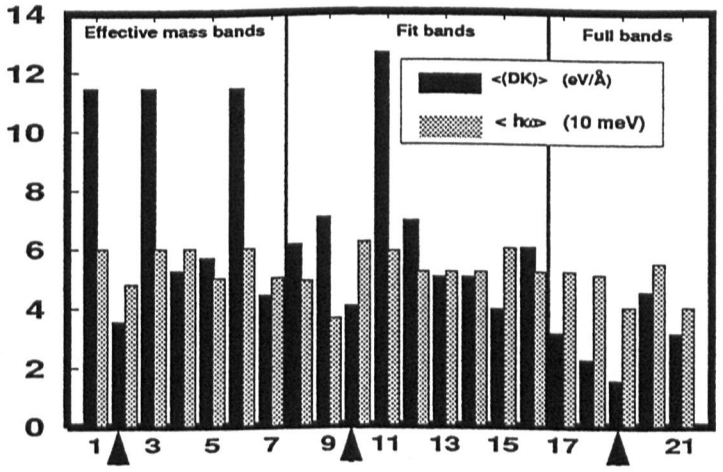

Figure 3. Effective intervalley deformation potential and effective intervalley phonon energy for each data set.

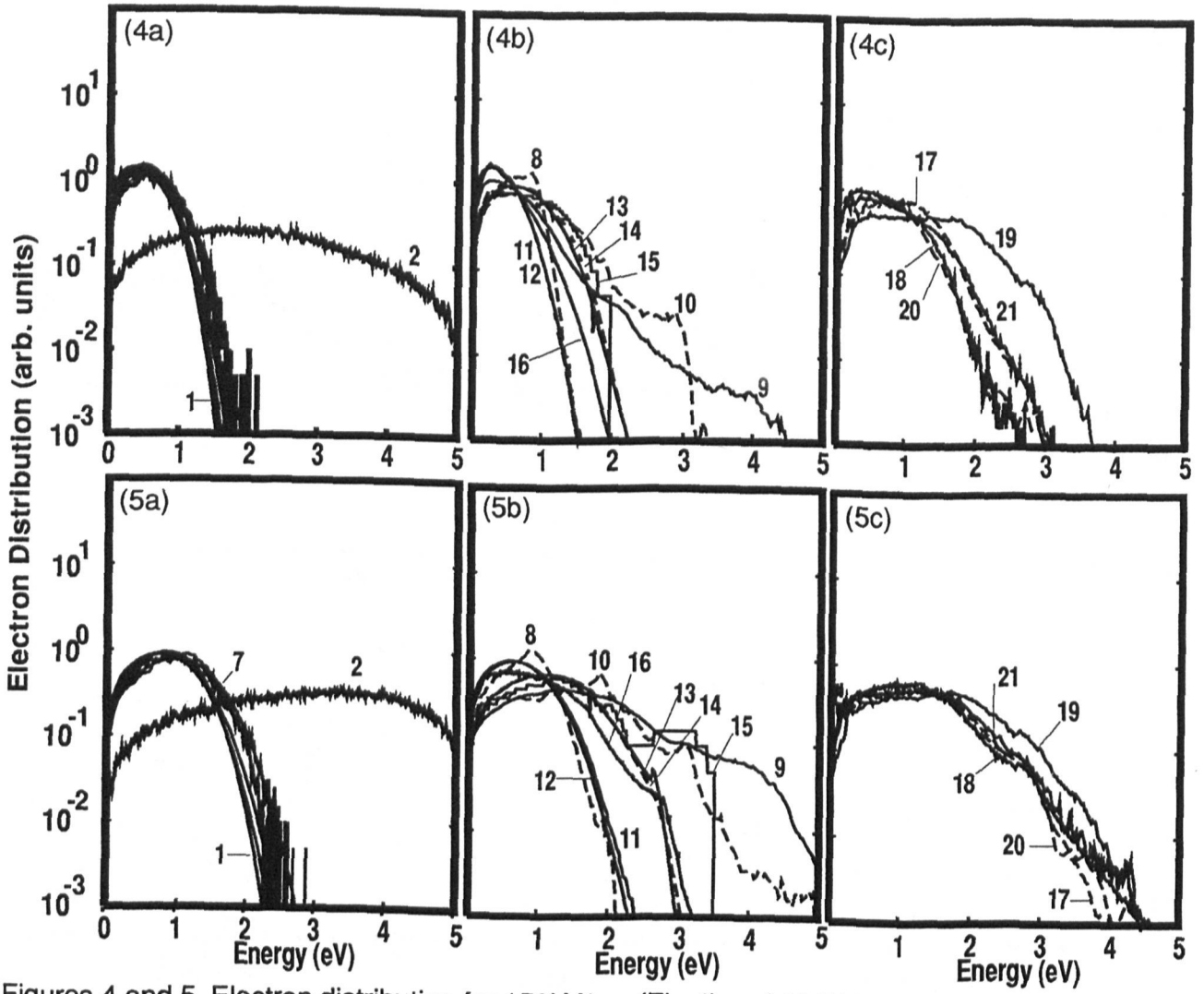

Figures 4 and 5. Electron distribution for 150kV/cm (Fig.4) and 300kV/cm (Fig.5), for (a) effective mass band models, (b) fit-band models, and (c) full-band models.

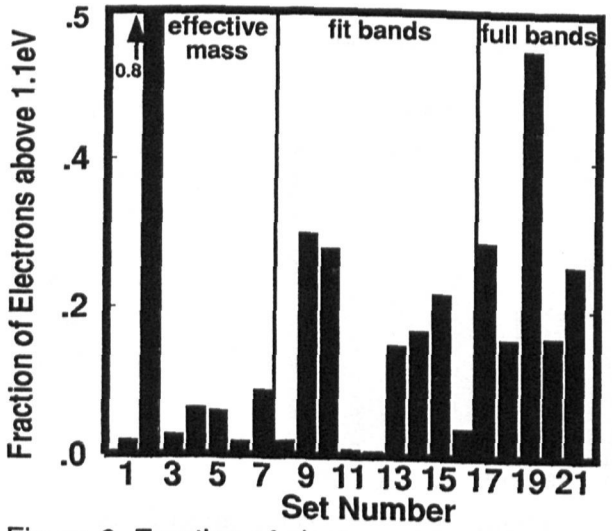

Figure 6. Fraction of electrons above 1.1eV; applied electric field = 150kV/cm.

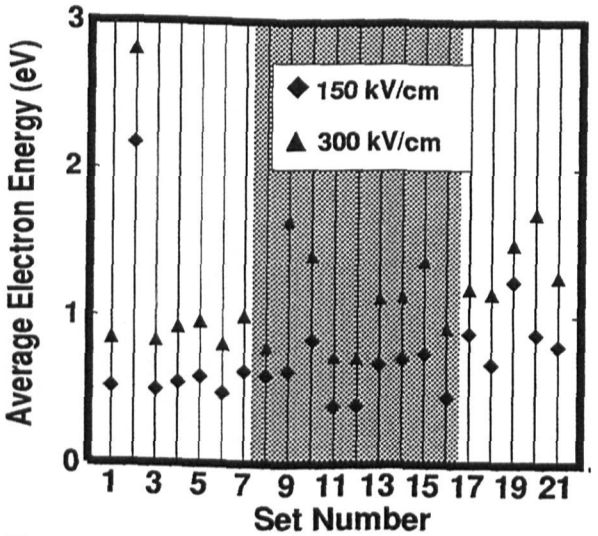

Figure 7. Average electron energy for each set at 150 and 300kV/cm.